

Search for the Blazhko effect in field RR Lyrae stars using LINEAR and ZTF light curves

Ema Donev¹ and Željko Ivezić²

¹ XV. Gymnasium (MIOC), Jordanovac 8, 10000, Zagreb, Croatia, e-mail: emadonev@icloud.com

² Department of Astronomy and the DiRAC Institute, University of Washington, 3910 15th Avenue NE, Seattle, WA, USA e-mail: ivezic@uw.edu

October 2024

ABSTRACT

We analyzed the incidence and properties of RR Lyrae stars that show evidence for amplitude and phase modulation (the so-called Blazhko Effect) in a sample of $\sim 3,000$ stars with LINEAR and ZTF light curve data. A preliminary subsample of about ~ 240 stars was algorithmically pre-selected using various data quality and light curve statistics, and then 139 stars were confirmed visually as displaying the Blazhko effect. This sample places a lower limit of 5% for the incidence of the Blazhko Effect in field RR Lyrae stars. Although close to 8,000 Blazhko stars were discovered or confirmed in the Galactic bulge and LMC/SMC by the OGLE-III survey, only about 200 stars have been reported in all field RR Lyrae stars studies to date; the sample presented here nearly doubles the number of field RR Lyrae stars displaying the Blazhko effect. With time-resolved photometry expected from LSST, a similar analysis will be performed for RR Lyrae stars in the southern sky and we anticipate a higher fraction of discovered Blazhko stars due to better sampling and superior photometric quality.

Key words. Variable stars — RR Lyrae stars — Blazhko Effect

1. Introduction

RR Lyrae stars are pulsating variable stars with periods in the range of 3–30 hours and large amplitudes that increase towards blue optical bands (e.g., in the SDSS g band from 0.2 mag to 1.5 mag; Sesar et al. 2010). For comprehensive reviews of RR Lyrae stars, we refer the reader to Smith (1995) and Catelan (2009).

RR Lyrae stars often exhibit amplitude and phase modulation, or the so-called Blazhko effect¹ (hereafter, “Blazhko stars”). For examples of well-sampled observed light curves showing the Blazhko effect, see, e.g., Kepler data shown in Figures 1 and 2 from Benkő et al. (2010). The Blazhko effect has been known for a long time (Blažko 1907), but its detailed observational properties and theoretical explanation of its causes remain elusive (Kolenberg 2008; Kovács 2009; Szabó 2014). Various proposed models for the Blazhko effect, and principal reasons why they fail to explain observations, are summarized in Kovacs (2016).

A part of the reason for the incomplete observational description of the Blazhko effect is difficulties in discovering a large number of Blazhko stars due to temporal baselines that are too short and insufficient number of observations per object (Kovacs 2016; Hernitschek & Stassun 2022). With the advent of modern sky surveys, several studies reported large increases in the number of known Blazhko stars, starting with a sample of about 700 Blazhko stars discovered by the MACHO survey towards the LMC (Alcock et al. 2003) and about 500 Blazhko stars discovered by the OGLE-II survey towards the Galactic bulge (Mizerski 2003). Most recently, about 4,000 Blazhko stars were discovered in the LMC and SMC (Soszyński et al. 2009, 2010), and

an additional $\sim 3,500$ stars were discovered in the Galactic bulge (Soszyński et al. 2011), both by the OGLE-III survey. Nevertheless, discovering the Blazhko effect in field RR Lyrae stars that are spread over the entire sky remains a much harder problem: only about 200 Blazhko stars in total from all the studies of field RR Lyrae stars have been reported so far (see Table 1 in Kovacs 2016).

Here, we report the results of a search for the Blazhko effect in a sample of $\sim 3,000$ field RR Lyrae stars with LINEAR and ZTF light curve data. A preliminary subsample of about ~ 240 stars was selected using various light curve statistics, and then ~ 140 stars were confirmed visually as displaying the Blazhko effect. This new sample greatly increases the number of known field RR Lyrae stars that exhibit the Blazhko effect. In §2 and §3 we describe our datasets and analysis methodology, and in §4 we present our analysis results. Our main results are summarized and discussed in §5.

2. Data Description and Period Estimation

Analysis of field RR Lyrae stars requires a sensitive time-domain photometric survey over a large sky area. For our starting sample, we used $\sim 3,000$ field RR Lyrae stars with light curves obtained by the LINEAR asteroid survey. In order to study long-term changes in light curves, we also utilized light curves obtained by the ZTF survey which monitored the sky ~ 15 years after LINEAR. The combination of LINEAR and ZTF provided a unique opportunity to systematically search for the Blazhko effect in a large number of field RR Lyrae stars.

¹ The Blazhko effect was discovered by Lidiya Petrovna Tseraskaya and first reported by Sergey Blazhko.

57 We first describe each dataset in more detail, and then introduce our analysis methods. All our analysis code, written in
 58 Python, is available on GitHub².
 59

60 2.1. LINEAR Dataset

61 The properties of the LINEAR asteroid survey and its photometric re-calibration based on SDSS data are discussed in Sesar
 62 et al. (2011). Briefly, the LINEAR survey covered about 10,000
 63 deg² of the northern sky in white light (no filters were used, see
 64 Figure 1 in Sesar et al. 2011), with photometric errors ranging
 65 from ~ 0.03 mag at an equivalent SDSS magnitude of $r = 15$ to
 66 0.20 mag at $r \sim 18$. Light curves used in this work include, on
 67 average, 270 data points collected between December 2002 and
 68 September 2008.

69 A sample of 7,010 periodic variable stars with $r < 17$ discovered
 70 in LINEAR data were robustly classified by Palaversa et al.
 71 (2013), including about $\sim 3,000$ field RR Lyrae stars of both ab
 72 and c type, detected to distances of about 30 kpc (Sesar et al.
 73 2013). The sample used in this work contains 2196 ab-type and
 74 745 c-type RR Lyrae, selected using classification labels and the
 75 *gi* color index from Palaversa et al. (2013). The LINEAR light
 76 curves, augmented with IDs, equatorial coordinates, and other
 77 data, were accessed using the astroML Python module³ (Van-
 78 derPlas et al. 2012).

80 2.2. ZTF Dataset

81 The Zwicky Transient Factory (ZTF) is an optical time-domain
 82 survey that uses the Palomar 48-inch Schmidt telescope and a
 83 camera with 47 deg² field of view (Bellm et al. 2019). The
 84 dataset analyzed here was obtained with SDSS-like *g*, *r*, and *i*
 85 band filters. Light curves for objects in common with the LIN-
 86 EAR RR Lyrae sample typically have smaller random photomet-
 87 ric errors than LINEAR light curves because ZTF data are deeper
 88 (compared to LINEAR, ZTF data have about 2–3 magnitudes
 89 fainter 5 σ depth). ZTF data used in this work were collected be-
 90 tween February 2018 and December 2023, on average about 15
 91 years after obtaining LINEAR data.

92 The ZTF dataset for this project was created by selecting
 93 ZTF IDs with matching equatorial coordinates to a correspond-
 94 ing LINEAR ID of an RR Lyrae star. This process used the
 95 *ztfquery* function, which searched the coordinates in the ZTF
 96 database within 3 arcsec from the LINEAR position. The result-
 97 ing sample consisted of 2857 RR Lyrae stars with both LINEAR
 98 and ZTF data. The fractions of RRab and RRc type RR Lyrae in
 99 this sample, 71% RRab and 29% RRc type, are consistent with
 100 results from other surveys (e.g., Sesar et al. 2010).

101 2.3. Period Estimation

102 The first step of our analysis is estimating best-fit periods, sepa-
 103 rately for LINEAR and ZTF datasets. We used the Lomb-Scargle
 104 method (Vanderplas 2015) as implemented in *astropy* (Astropy
 105 Collaboration et al. 2018). The period estimation used 3 Fourier
 106 components and a two-step process: an initial best-fit frequency
 107 was determined using the *autopower* frequency grid option and
 108 then the power spectrum was recomputed around the initial fre-
 109 quency using an order of magnitude smaller frequency step. In
 110 case of ZTF, we estimated period separately for each available

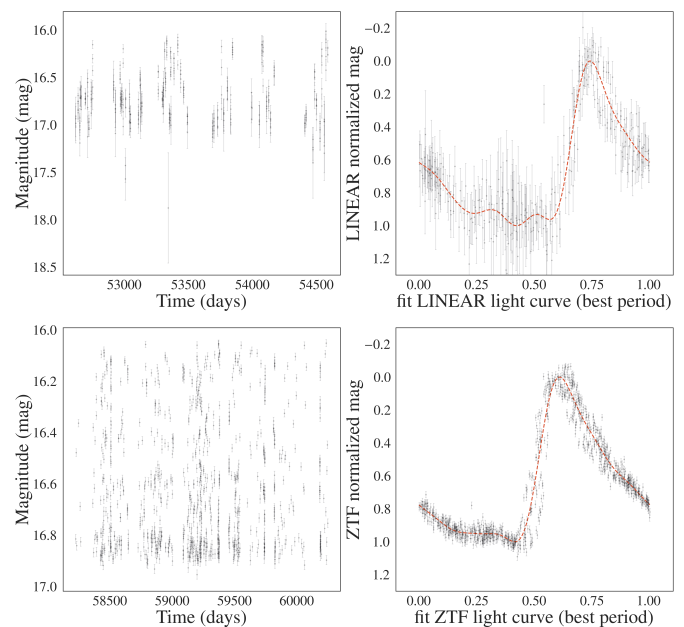


Fig. 1. An example of a (Blazhko?) star with LINEAR (top row) and ZTF (bottom row) light curves (left panels, data points with “error bars”), phased light curves normalized to the 0–1 range (right panels, data points with “error bars”), with their best-fit models shown by dashed lines.

111 passband and adopted their mean value. Once the best-fit mean
 112 value was determined, a best-fit model for the phased light curve was
 113 computed using 6 Fourier components. Fig 1 shows an exam-
 114 ple of a star with LINEAR and ZTF light curves, phased light
 115 curves, and their best-fit models.

116 We found excellent agreement between the best-fit periods
 117 estimated separately from LINEAR and ZTF light curves. The
 118 median of their ratio is unity within 2×10^{-6} and the robust stan-
 119 dard deviation of their ratio is 2×10^{-5} . With a median sample
 120 period of 0.56 days, the implied scatter of period difference is
 121 about 1.0 sec.

122 Given on average about 15 years between LINEAR and ZTF
 123 data sets, and a typical period of 0.56 days, this time difference
 124 corresponds to about 10,000 oscillations. With a fractional per-
 125 iod uncertainty of 2×10^{-5} , LINEAR data can predict the phase
 126 of ZTF light curve with an uncertainty of 0.2. Therefore, for a
 127 robust detection of light curve phase modulation, each data set
 128 must be analyzed separately. On the other hand, amplitude mod-
 129 ulation can be detected on time scales as long as 15 years, as
 130 discussed in the following section.

131 3. Analysis Methodology: Searching for the Blazhko 132 Effect

133 Given the two sets of light curves from LINEAR and ZTF, we
 134 searched for amplitude and phase modulation, either during the
 135 5–6 years of data taking by each survey, or during the average
 136 span of 15 years between the two surveys. Starting with a sam-
 137 ple of 2857 RR Lyrae stars, we pre-selected a smaller sample
 138 that was inspected visually (see below for details). We also re-
 139 quired at least 250 LINEAR data points and 40 ZTF data points
 140 (per band) in analyzed light curves. We used two pre-selection
 141 methods that are sensitive to different types of light curve mod-
 142 ulation: direct light curve analysis and periodogram analysis, as
 143 follows.

² https://github.com/emadonev/var_stars

³ For an example of light curves, see https://www.astroml.org/book_figures/chapter10/fig_LINEAR_LS.html

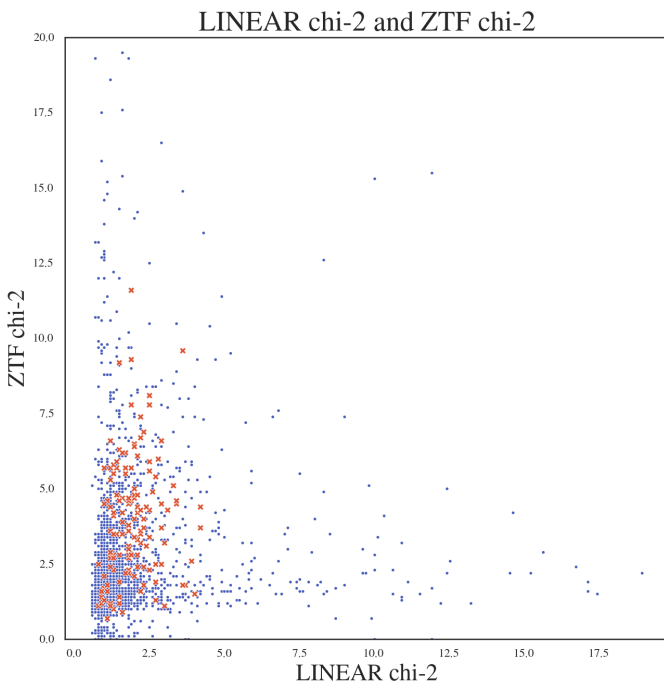


Fig. 2. A diagram constructed with the two sets of χ^2_{dof} values, for LINEAR and ZTF data sets, where blue symbols represents all RR Lyrae stars and the red symbols are the final sample of Blazhko stars.

3.1. Direct Light Curve Analysis

Given statistically correct period, amplitude and light curve shape estimates, as well as data being consistent with reported (presumably Gaussian) uncertainty estimates, the χ^2 per degree of freedom gives a quantitative assessment of the "goodness of fit",

$$\chi^2_{dof} = \frac{1}{N_{dof}} \sum \frac{(d_i - m_i)^2}{\sigma_i^2}. \quad (1)$$

Here, d_i are measured light curve data values at times t_i , and with associated uncertainties σ_i , m_i are best-fit models at times t_i , and N_{dof} is the number of degrees of freedom, essentially the number of data points. In the absence of any light curve modulation, the expected value of χ^2_{dof} is unity, with a standard deviation of $\sqrt{2/N_{dof}}$. If $\chi^2_{dof} - 1$ is many times larger than $\sqrt{2/N_{dof}}$, it is unlikely that data d_i were generated by the assumed (unchanging) model m_i . Of course, χ^2_{dof} can also be large due to underestimated measurement uncertainties σ_i , or to occasional non-Gaussian measurement error (the so-called outliers).

Therefore, to search for signatures of the Blazhko effect, manifested through statistically unlikely large values of χ^2_{dof} , we computed χ^2_{dof} separately for LINEAR and ZTF data (see Figure 2). Using the two sets of χ^2_{dof} values, we algorithmically pre-selected a sample of candidate Blazhko stars for further visual analysis of their light curves. The visual analysis is needed to confirm the expected Blazhko behavior in observed light curves, as well as to identify cases of data problems, such as photometric outliers.

We used a simple scoring algorithm, optimized through trial and error, such that for LINEAR the range $1.8 < \chi^2_{dof} < 3.0$ was worth 2 points and $\chi^2_{dof} > 3.0$ worth 3 points, while for ZTF $2.0 < \chi^2_{dof} < 4.0$ and $\chi^2 > 4.0$ were the analogous limits.

In addition, we also considered normalized period differences (dP) and amplitude differences (dA) and assigned: 2 points for $0.00002 < dP < 0.00005$ and 4 points for $dP > 0.00005$; 1 point for $0.05 < dA < 0.15$ and 2 points for $dA > 0.15$. A star could score a maximum of 12 points, and a minimum of 5 points was required for further visual analysis.

The sample pre-selected using this method includes 189 stars. For most selected stars, the χ^2_{dof} values were larger for the ZTF data because the ZTF photometric uncertainties are smaller than for the LINEAR data set. Fig. 3 summarizes the selection criteria and the resulting numbers of selected stars for each criterion and their combinations.

3.2. Periodogram Analysis

When light curve modulation is due to double-mode oscillation with two similar oscillation frequencies (periods), it is possible to recognize its signature in the periodogram computed as part of the Lomb-Scargle analysis. Depending on various details, such as data sampling and the exact values of periods, amplitudes, this method may be more efficient than direct light curve analysis.

A sum of two *sine* functions with same amplitudes and with frequencies f_1 and f_2 can be rewritten using trigonometric equalities as

$$y(t) = 2 \cos(2\pi \frac{f_1 - f_2}{2} t) \sin(2\pi \frac{f_1 + f_2}{2} t). \quad (2)$$

We can define

$$f_o = \frac{f_1 + f_2}{2}, \quad (3)$$

and

$$\Delta f = |\frac{f_1 - f_2}{2}|, \quad (4)$$

with $\Delta f \ll f_o$ when f_1 and f_2 are similar. The fact that Δf is much smaller than f_o means that the period of the *cos* term is much larger than the period of the basic oscillation (f_o). In other words, the *cos* term acts as a slow amplitude modulation of the basic oscillation. When the amplitudes of two *sine* functions are not equal, the results are more complicated but the basic conclusion about amplitude modulation remains. When the power spectrum of $y(t)$ is constructed, it will show 3 peaks: the main peak at f_o and two more peaks at frequencies $f_o \pm \Delta f$. We used this fact to construct an algorithm for automated searching for the evidence of amplitude modulation. Fig 4 compares the theoretical periodogram produced by interference beats with our algorithm's periodogram, signifying that local Blazhko peaks are present in real data.

After the strongest peak in the Lomb-Scargle periodogram is found at frequency f_o , we search for two equally distant local peaks at frequencies f_- and f_+ , with $f_- < f_o < f_+$. The side-band peaks can be highly asymmetric Alcock et al. (2003) and observed periodograms can sometimes be much more complex Szczygieł & Fabrycky (2007). We fold the periodogram through the main peak at f_o , multiply the two branches and then search for the strongest peaks in the resulting folded periodogram that is statistically more significant than the background noise. The background noise is computed as the scatter of the folded periodogram estimated from the interquartile range. We require a "signal-to-noise" ratio of at least 5, as well as the peak strength of at least 0.05. If such a peak is found, and it doesn't correspond

Analysis of blazhko star metrics for RR Lyrae

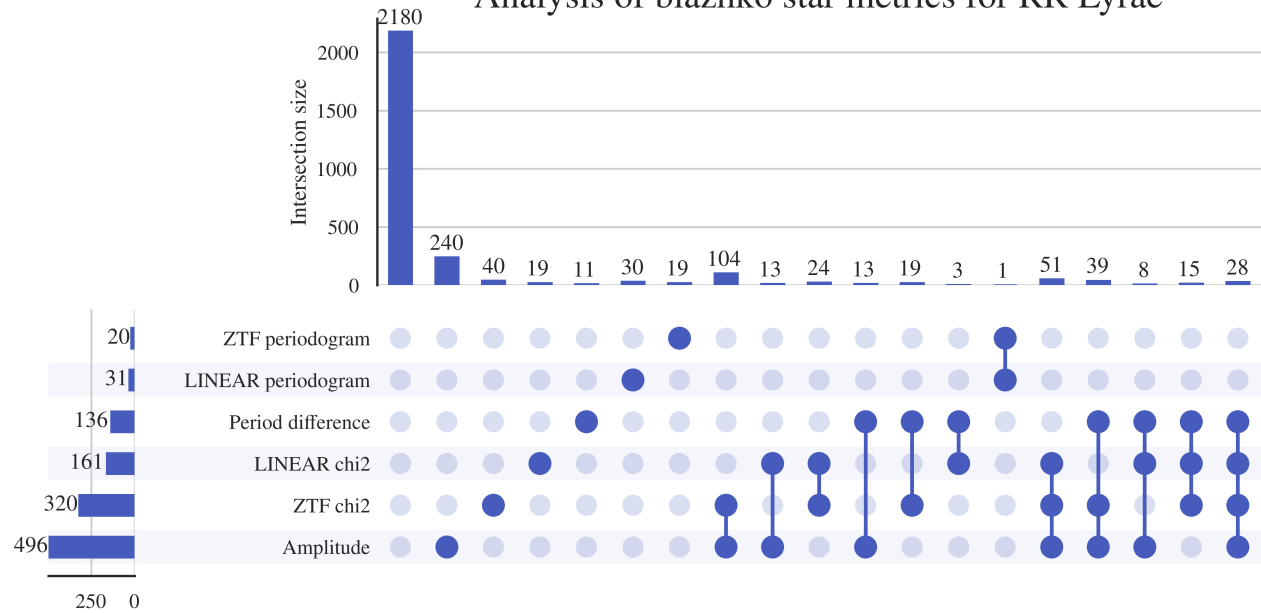


Fig. 3. The figure shows selection criteria and the resulting numbers of pre-selected Blazhko star candidates for each criterion and their combinations. The dots represent each case a star can occupy, where every solid dot is a specific criterion that is satisfied. Connections between solid dots represent stars which satisfy multiple criteria. Each dot combination has its own count, represented by the horizontal countplot. The vertical countplot shows the total number of stars that satisfy one criteria (union of all cases).

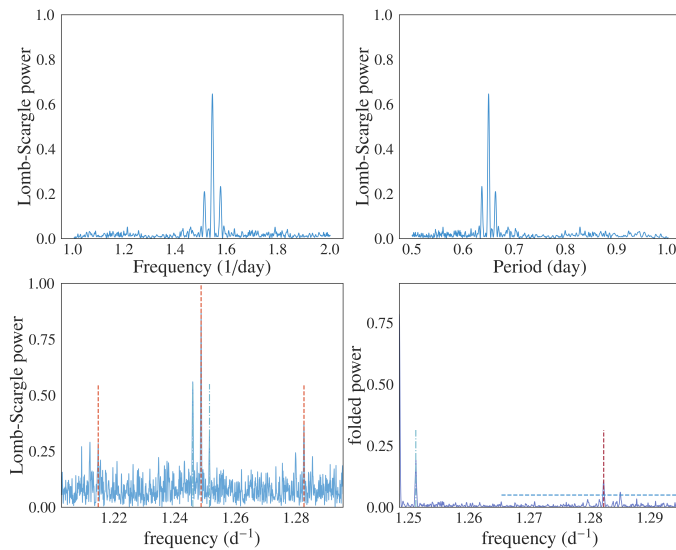


Fig. 4. The top two panels show a simulated periodogram for a sum of two *sine* functions with similar frequencies – the central peak corresponds to their mean. The bottom left panel shows a periodogram for an observed LINEAR light curve, and the bottom right panel shows its folded version. The vertical dashed lines show the three frequencies identified by the algorithm described in text.

mag (Szczygieł & Fabrycky 2007). In this work, we selected a smaller Blazhko range due to the limitations of our data: 30–325 days. With this additional constraint, we selected 51 candidate Blazhko stars, with one star already included in the sample of 189 stars described in preceding section. Fig 5 shows an example where two very prominent peaks were identified in the LINEAR

231
232
233
234
235
236
237

3.2.1. Visual Confirmation

The sample pre-selected for visual analysis includes 239 RR Lyrae stars (189 + 51, with one star selected twice), or 8.4% of the starting LINEAR-ZTF sample. Visual analysis included the following standard steps (e.g., Jurcsik et al. 2009):

1. The shape of the phased light curves and scatter of data points around the best-fit model were examined for signatures of anomalous behavior indicative of the Blazhko effect. Fig. 6 shows an example of such behavior where the ZTF data and fit show multiple coherent data point sequences offset from the best-fit mean model.
2. Full light curves were inspected for their repeatability between observing seasons (Fig. 7). This step was sensitive to amplitude modulations with periods of the order a year or longer.
3. The phased light curves normalized to unit amplitude were inspected for their repeatability between observing seasons. This step was sensitive to phase modulations of a few percent or larger on time scales of the order a year or longer. Fig. 8 shows an example of a Blazhko star where season-to-season phase (and amplitude) modulations are seen in both the LINEAR data and (especially) the ZTF data.

After visually analyzing the starting sample of 239 Blazhko candidates, we visually confirmed expected Blazhko behavior for 136 stars (112 out of 189 and 24 out of 50). LINEAR IDs

224 to yearly alias, we select the star as a candidate Blazhko star and
225 compute its Blazhko period as

$$226 P_{BL} = |f_{-,+} - f_0|^{-1},$$

227 where $f_{-,+}$ means the Blazhko sideband frequency with a higher
228 amplitude is chosen.

229 The observed Blazhko periods range from 3 to 3,000 days,
230 and Blazhko amplitudes range from 0.01 mag to about 0.3

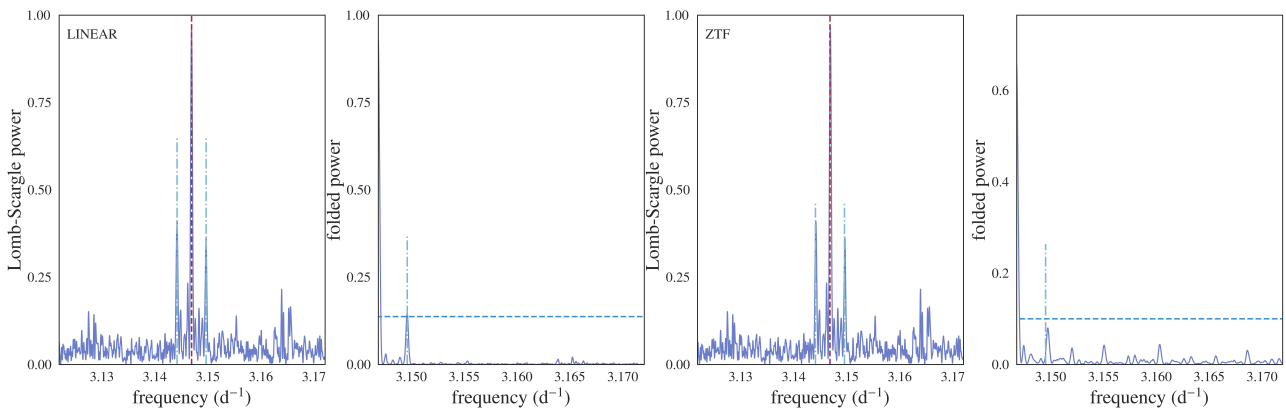


Fig. 5. Phase 2 of visual analysis of Blazhko candidates. XXX Are these LINEAR and ZTF periodograms? Is this figure a bit redundant with the previous figure?

and other characteristics for confirmed Blazhko stars are listed in Table 1 (Appendix A). Statistical properties of the selected sample of Blazhko stars are discussed in detail in the next section.

STOPPED HERE

4. Results

UNFINISHED

Starting with a sample of 2857 field RR Lyrae stars with both LINEAR and ZTF data, we found 136 stars exhibiting convincing Blazhko effect. In Appendix A, the reader can find all of the Blazhko stars and some elementary data describing each star.

Another important note highlighting the difficulty of finding Blazhko stars is that the absolute Blazhko frequency difference from the main frequency is approximately 0.028 d^{-1} . Also, the average period difference between LINEAR and ZTF in Blazhko stars was around 0.0001 days. These minimal differences require precise observations over a long temporal baseline.

Finally, we have discovered that in some Blazhko stars, the effect cannot be detected ten years later or beforehand. When comparing LINEAR and ZTF data, some pairs have the effect present in only one dataset and others in both. This finding could mean that the Blazhko effect is not always present and gives us a clue about its mechanism. However, the precision of data is also a factor for consideration.

5. Discussion and Conclusions

UNFINISHED

The reported incidence rates for the Blazhko effect range from 5% (Szczygieł & Fabrycky 2007) to 60% (Szabó et al. 2014). For a relatively small sample of 151 stars with Kepler data, a claim has been made that essentially every RR Lyrae star exhibits modulated light curve (Kovacs 2018). The difference in Blazhko incidence rates for the two most extensive samples, obtained by the OGLE-III survey for the Large Magellanic Cloud (LMC, 20% out of 17,693 stars; Soszyński et al. 2009). Moreover, the Galactic bulge (30% out of 11,756 stars; Soszyński et al. 2011) indicates a possible variation of the Blazhko incidence rate with underlying stellar population properties. In this work, 4.67% of the original RR Lyrae dataset are Blazhko stars. Since our sample size is considerable, we conclude that the incidence rate of Blazhko stars in our work is representative and aligns with other works. We theorize that the difference in incidence rates occurs due to varying data precision, the temporal

baseline length, and differences in visual or algorithmic analysis. We also conclude that our algorithm's success rate in finding 136 out of 239 potential Blazhko stars is 57%. This high number indicates that the algorithm is very successful and can be used and refined further for efficient Blazhko star selection.

For future research, we would like to explore the final finding and find a connection or a factor that might give rise to a mechanism that explains the Blazhko effect. The project is an excellent example of automatizing the search for Blazhko stars. It can further be improved by training a neural network to replace visual analysis, and our current algorithms can be improved with other models. This work can provide a base for finding more Blazhko stars for the future Vera Rubin observatory. The Legacy Survey of Space and Time (LSST; Ivezić et al. 2019) will be an excellent survey for studying Blazhko effect (Hernitschek & Stassun 2022) because it will have both a long temporal baseline (10 years) and a large number of observations per object (nominally 825; LSST Science Requirements Document⁴).

Claim from the abstract: With time-resolved photometry expected from LSST, a similar analysis will be performed for RR Lyrae stars in the southern sky and we anticipate a higher fraction of discovered Blazhko stars due to better sampling and superior photometric quality. Support with this quote:

the incidence rate of the Blazhko effect increases with sensitivity to small-amplitude modulation, and thus with photometric data quality (Jurcsik et al. 2009).

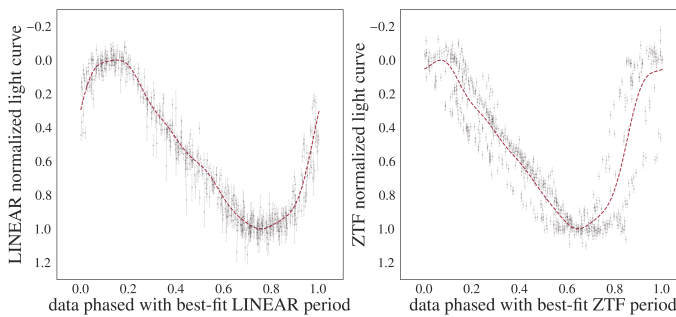
We confirm that the light curve modulation can be unstable, as discussed by Jurcsik et al. (2009)

From Jurcsik et al. (2009): A sample of 30 RRab stars was extensively observed, and light-curve modulation was detected in 14 cases. The 47 per cent occurrence rate of the modulation is much larger than any previous estimate.

Acknowledgements. We thank Mathew Graham for providing *ztfquery* code example to us. Ž.I. acknowledges funding by the Fulbright Foundation and thanks the Ruđer Bošković Institute (Zagreb, Croatia) for hospitality. Based on observations obtained with the Samuel Oschin Telescope 48-inch and the 60-inch Telescope at the Palomar Observatory as part of the Zwicky Transient Facility project. ZTF is supported by the National Science Foundation under Grants No. AST-1440341 and AST-2034437 and a collaboration including current partners Caltech, IPAC, the Weizmann Institute of Science, the Oskar Klein Center at Stockholm University, the University of Maryland, Deutsches Elektronen-Synchrotron and Humboldt University, the TANGO Consortium of Taiwan, the University of Wisconsin at Milwaukee, Trinity College Dublin, Lawrence Livermore National Laboratories, IN2P3, University of Warwick, Ruhr University Bochum, Northwestern University and former partners the University of Washington, Los Alamos National Laboratories, and Lawrence Berkeley National

⁴ Available as ls.st/srd

STAR 1 from 136



LINEAR period chi robust: 1.2, LINEAR mean period chi robust: 1.3
ZTF period chi robust: 1.1, ZTF mean period chi robust: 1.0
LINEAR period chi: 1.8, LINEAR mean period chi: 1.9
ZTF period chi: 0.8, ZTF mean period chi: 1.0
LINEAR period: 0.372376, ZTF period: 0.372384, Period difference: 2e-05
Average LINEAR magnitude: 15.21
LINEAR amplitude: 0.42, ZTF amplitude: 0.59

Fig. 6. An illustration of visual analysis of phased light curves for the selected Blazhko candidates. The left panel shows LINEAR data and the right panel shows ZTF data (symbols with “error bars”). The dashed lines are best-fit models. The numbers listed on the right side were added to aid visual analysis. Note multiple coherent data point sequences offset from the best-fit mean model in the right panel.

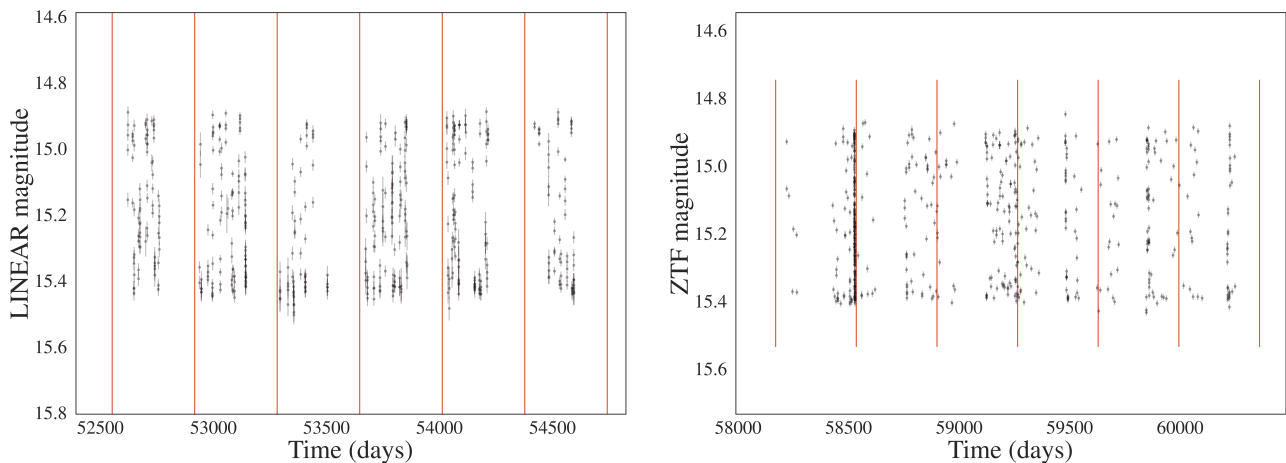


Fig. 7. Visual analysis of full light curves for the selected Blazhko candidates with emphasis on their repeatability between observing seasons, marked with vertical lines (left: LINEAR data; right: ZTF data).

351 Laboratories. Operations are conducted by COO, IPAC, and UW. The LINEAR
352 program is funded by the National Aeronautics and Space Administration at MIT
353 Lincoln Laboratory under Air Force Contract FA8721-05-C-0002. Opinions, in-
354 terpretations, conclusions and recommendations are those of the authors and are
355 not necessarily endorsed by the United States Government.

References

- | | |
|--|-----|
| Alcock, C., Alves, D. R., Becker, A., et al. 2003, ApJ, 598, 597 | 357 |
| Astropy Collaboration, Price-Whelan, A. M., Sipőcz, B. M., et al. 2018, AJ, 156, 123 | 358 |
| Bellm, E. C., Kulkarni, S. R., Graham, M. J., et al. 2019, PASP, 131, 018002 | 359 |
| Benkő, J. M., Kolenberg, K., Szabó, R., et al. 2010, MNRAS, 409, 1585 | 360 |
| Blažko, S. 1907, Astronomische Nachrichten, 175, 325 | 361 |
| Catelan, M. 2009, Ap&SS, 320, 261 | 362 |
| Hernitschek, N. & Stassun, K. G. 2022, ApJS, 258, 4 | 363 |
| Ivezić, Ž., Kahn, S. M., Tyson, J. A., et al. 2019, ApJ, 873, 111 | 364 |
| Jurcsik, J., Sődör, Á., Szeidl, B., et al. 2009, MNRAS, 400, 1006 | 365 |
| Kolenberg, K. 2008, in Journal of Physics Conference Series, Vol. 118, Journal of Physics Conference Series (IOP), 012060 | 366 |
| Kovács, G. 2009, in American Institute of Physics Conference Series, Vol. 1170, Stellar Pulsation: Challenges for Theory and Observation, ed. J. A. Guzik & P. A. Bradley, 261–272 | 367 |
| Kovacs, G. 2016, Communications of the Konkoly Observatory Hungary, 105, 61 | 368 |
| Kovacs, G. 2018, A&A, 614, L4 | 369 |
| Mizerski, T. 2003, Acta Astron., 53, 307 | 370 |
| Palaversa, L., Ivezić, Ž., Eyer, L., et al. 2013, AJ, 146, 101 | 371 |
| Sesar, B., Ivezić, Ž., Grammer, S. H., et al. 2010, ApJ, 708, 717 | 372 |
| Sesar, B., Ivezić, Ž., Stuart, J. S., et al. 2013, AJ, 146, 21 | 373 |
| Sesar, B., Stuart, J. S., Ivezić, Ž., et al. 2011, AJ, 142, 190 | 374 |
| Smith, H. A. 1995, Cambridge Astrophysics Series, 27 | 375 |
| Soszyński, I., Dziembowski, W. A., Udalski, A., et al. 2011, Acta Astron., 61, 1 | 376 |
| Soszyński, I., Udalski, A., Szymański, M. K., et al. 2010, Acta Astron., 60, 165 | 377 |
| Soszyński, I., Udalski, A., Szymański, M. K., et al. 2009, Acta Astron., 59, 1 | 378 |
| Szabó, R. 2014, in IAU Symposium, Vol. 301, Precision Asteroseismology, ed. J. A. Guzik, W. J. Chaplin, G. Handler, & A. Pigulski, 241–248 | 379 |
| Szabó, R., Benkő, J. M., Paparó, M., et al. 2014, A&A, 570, A100 | 380 |
| Szczygiel, D. M. & Fabrycky, D. C. 2007, MNRAS, 377, 1263 | 381 |
| Vanderplas, J. 2015, gatspy: General tools for Astronomical Time Series in Python | 382 |
| VanderPlas, J., Connolly, A. J., Ivezić, Z., & Gray, A. 2012, in Proceedings of Conference on Intelligent Data Understanding (CIDU), 47–54 | 383 |

Seasons for: 7048826

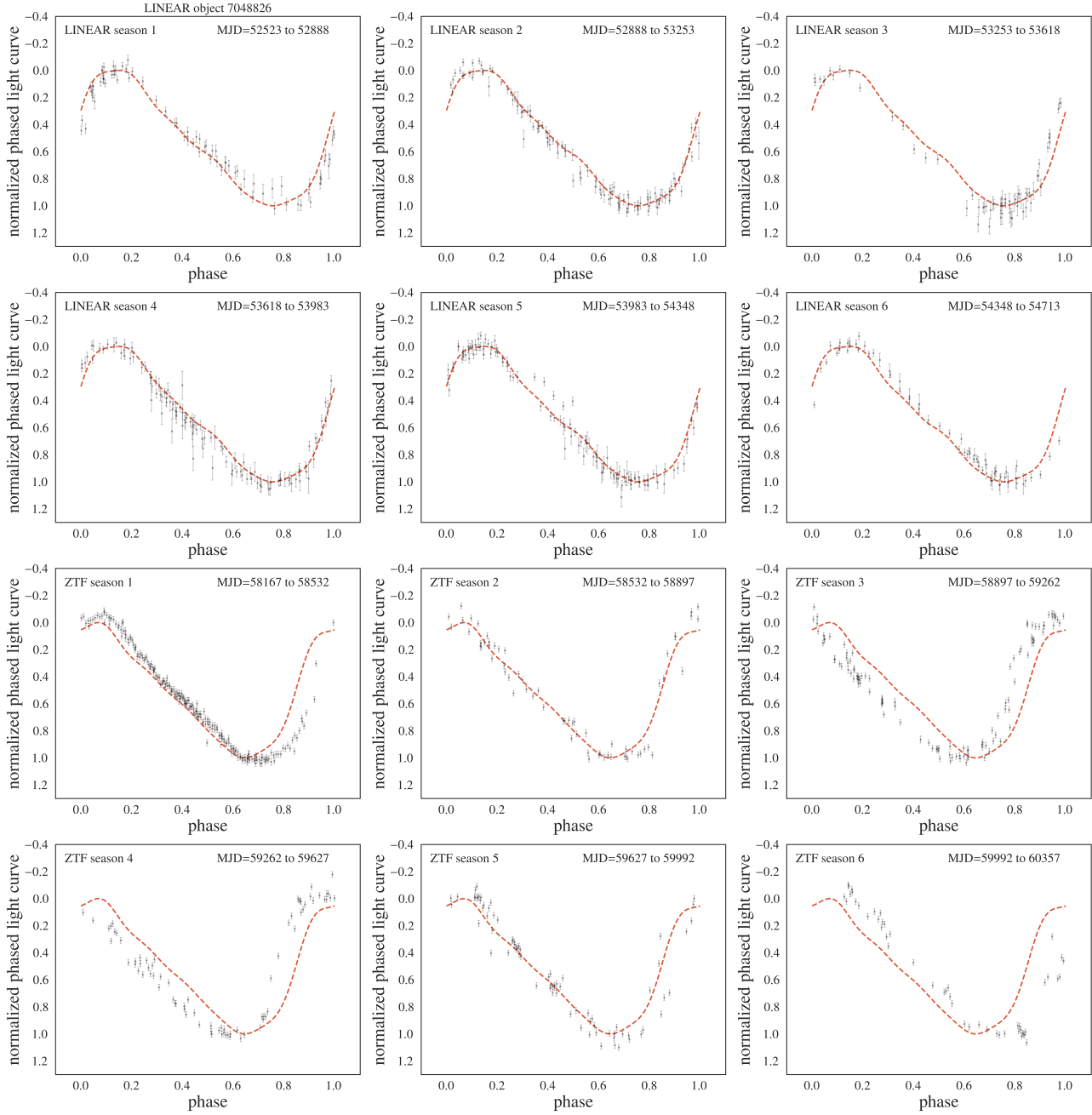


Fig. 8. The phased light curves normalized to unit amplitude are shown for single observing seasons and compared to the mean best-fit models (top six panels: LINEAR data; bottom six panels: ZTF data). Season-to-season phase and amplitude modulations are seen in both the LINEAR and the ZTF data.

392 **Appendix A: Full table of results**

393 Here we present all the confirmed Blazhko stars with their LINEAR IDs, equatorial coordinates, and calculated periods and χ^2
 394 values.

LINEAR ID	RA	DEC	LINEAR period	ZTF period	LINEAR chi-2	ZTF chi-2
523832	207.529404	33.706001	0.372376	0.372384	1.20	1.10
1240665	206.202469	34.058662	0.632528	0.632522	3.00	1.10
1736308	206.096115	36.648674	0.555848	0.555843	1.30	1.00
2669011	206.229523	38.758453	0.591153	0.591151	1.10	0.70
2742032	207.355225	39.589951	0.629676	0.629692	0.90	1.40
2812086	206.805511	40.859066	0.646015	0.646000	3.00	3.20
3507643	206.557358	39.536449	0.801141	0.801132	1.60	0.90
5931160	207.177231	41.918797	0.664700	0.664708	0.80	1.10
6665721	206.020233	41.646141	0.643318	0.643325	1.00	1.70
17185566	206.387268	43.314617	0.614160	0.614169	1.50	1.90
22828215	206.657028	43.543236	0.574536	0.574535	1.50	1.40
29848	206.917358	44.971054	0.557020	0.557040	1.40	3.50
158779	207.772202	45.916824	0.609207	0.609189	1.60	3.90
263541	207.172470	45.713154	0.558218	0.558221	2.90	6.60
514883	206.594757	46.482040	0.557723	0.557737	1.70	5.50
737951	206.435547	45.881615	0.357023	0.357023	2.20	6.70
810169	169.297485	6.265203	0.465185	0.465212	2.10	2.80
924301	169.713531	6.963072	0.507503	0.507440	1.90	9.30
1092244	207.060974	5.649392	0.649496	0.649558	1.20	3.60
1244554	206.944962	5.346962	0.536875	0.536962	1.80	2.30
1307948	206.223587	6.741248	0.527474	0.527415	1.80	4.50
1332201	207.992432	-4.603579	0.580711	0.580731	1.60	4.20
1390653	207.220245	-3.214271	0.521867	0.521871	1.30	4.10
1435279	207.824600	-3.712567	0.381858	0.381860	2.10	4.20
1448299	206.582916	51.406654	0.606912	0.606940	2.70	5.40
1593736	169.096771	5.428976	0.592628	0.592650	1.20	5.70
1748058	207.353790	53.020401	0.310237	0.310176	1.40	5.70
1857382	206.026001	56.421604	0.566428	0.566407	2.70	2.50
1882354	207.117645	56.313797	0.695061	0.695029	1.50	2.80
2041979	206.848053	55.248009	0.653694	0.653639	1.20	5.30
2075949	207.733643	62.320267	0.477806	0.477666	1.60	4.70
2117028	207.188278	61.978554	0.591245	0.591243	2.20	3.50
2122319	206.210190	62.778843	0.359422	0.359424	2.10	6.10
2229607	207.042603	65.877083	0.575179	0.575211	1.20	4.40
2243683	206.780823	8.893113	0.579777	0.579803	3.10	4.30
2248787	206.407776	7.914382	0.563528	0.563539	2.10	2.40
2334384	206.454544	7.380644	0.555341	0.555333	2.00	6.50
2397296	168.680649	51.998081	0.488814	0.488836	1.20	6.60
2414841	206.101624	7.666218	0.559611	0.559592	1.70	5.70
2455568	168.211075	51.534416	0.594119	0.594092	2.00	2.10
2612592	207.693237	-5.975360	0.571562	0.571543	1.30	2.80
2653982	168.135025	51.014339	0.607082	0.607110	1.00	2.10
2766997	207.782440	-7.099904	0.289881	0.289943	1.80	3.60
2892940	209.495773	2.587467	0.539855	0.539896	1.30	4.20
3036295	209.338211	2.393512	0.629705	0.629714	1.80	2.20
3140139	208.758163	-0.100046	0.304590	0.304585	2.50	5.60
3183285	208.391159	0.479103	0.349653	0.349664	1.20	2.80
3196582	208.521881	0.740297	0.268017	0.268018	2.50	3.40
3196780	169.384384	53.303658	0.504148	0.504199	2.20	3.20
3294319	169.550766	53.459976	0.555460	0.555473	1.90	4.70
3437725	208.845749	12.514306	0.542457	0.542478	1.50	6.30
3591037	208.146072	14.167974	0.558643	0.558609	1.30	3.50
3941776	209.073120	13.401526	0.532222	0.532209	2.80	6.00
4101289	209.351425	13.537904	0.379225	0.379250	1.20	2.70
4586691	208.326218	15.475822	0.621459	0.621446	2.00	3.40
4804945	209.674210	16.421736	0.556172	0.556217	2.50	7.80
5421989	208.014435	18.561077	0.534510	0.534527	0.80	2.50

LINEAR ID	RA	DEC	LINEAR period	ZTF period	LINEAR chi-2	ZTF chi-2
6582265	209.421219	17.441139	0.691751	0.691749	2.90	3.70
6651516	208.909760	17.881287	0.308488	0.308496	1.30	5.80
6819457	209.491974	20.296762	0.436282	0.436265	3.60	9.60
6883239	208.333481	19.276327	0.563711	0.563712	2.90	2.50
6967017	208.406662	21.846382	0.529691	0.529677	2.30	6.90
7048826	208.492981	22.591896	0.317781	0.317790	1.40	5.90
7254801	209.648148	22.561989	0.561133	0.561071	1.30	5.50
7279621	208.915436	24.833937	0.415469	0.415467	1.90	4.60
7283275	208.409698	26.350325	0.543342	0.543331	2.20	3.60
7344401	209.188583	26.111385	0.330201	0.330226	1.80	2.70
7580734	209.349243	26.322409	0.314956	0.314957	2.00	4.00
7657340	208.098282	27.700201	0.495480	0.495493	2.30	4.00
7811366	208.457687	30.868412	0.489523	0.489521	2.00	4.70
7827663	208.047531	30.799057	0.390832	0.390832	3.40	4.50
7846640	209.106400	4.330462	0.551495	0.551518	1.50	9.20
8222011	209.258850	3.100914	0.350920	0.350914	2.00	4.80
8311517	208.212936	4.452833	0.523354	0.523359	1.80	3.60
8331094	208.446945	3.969552	0.267543	0.267549	2.10	3.30
8343291	208.919601	-2.689821	0.569785	0.569791	3.30	5.10
9063194	169.357468	57.331566	0.575781	0.575760	2.40	3.10
9236215	209.009872	-1.607280	0.352570	0.352572	1.80	2.80
9449335	209.488937	-2.928472	0.475720	0.475695	2.00	5.00
9532981	168.695602	60.104759	0.591000	0.591042	1.70	6.20
9918809	209.255295	-2.089725	0.479460	0.479509	1.90	11.60
9968431	209.717804	-2.437493	0.302266	0.302211	1.70	2.20
9979905	208.905365	31.572962	0.338739	0.338739	2.50	2.30
10030349	209.547668	32.537975	0.545073	0.545074	2.10	4.40
10260828	208.891602	32.249817	0.380655	0.380643	2.20	7.40
10814742	209.570526	31.039347	0.462687	0.462683	2.50	4.30
11215595	208.180191	33.574619	0.546960	0.546943	1.30	2.30
16991760	209.105652	33.977589	0.549098	0.549096	2.90	3.70
17247918	169.489120	59.391106	0.481867	0.481865	1.80	4.60
17275627	208.806717	33.957424	0.537775	0.537771	2.10	4.80
17302403	209.807205	35.285717	0.488261	0.488343	2.00	6.40
17544856	208.748581	36.859768	0.614297	0.614296	2.00	3.40
19775800	208.958618	36.484657	0.310856	0.310867	1.30	2.70
21488669	209.334930	37.248749	0.501644	0.501661	1.90	5.70
21556651	208.269577	38.000725	0.614826	0.614808	1.80	3.10
21619184	208.125366	37.095997	0.557343	0.557320	2.30	3.70
21806402	208.151657	39.543987	0.592081	0.592104	1.60	6.20
21874209	209.602371	40.245346	0.611295	0.611286	2.50	5.90
21967825	209.202347	39.452202	0.540607	0.540600	1.80	4.70
22244513	208.742203	41.386112	0.604149	0.604077	2.50	8.10
22319996	209.734711	42.773571	0.479505	0.479495	2.60	4.90
22518636	208.239105	41.299026	0.283996	0.283998	1.80	3.00
22959674	209.018127	41.835575	0.405333	0.405409	1.80	3.80
22980793	208.105713	44.400867	0.540348	0.540353	1.90	2.80
23135759	209.604721	45.746510	0.402730	0.402732	4.20	4.40
23148883	209.446594	45.757584	0.390130	0.390124	1.40	4.80
23184808	208.547745	47.825001	0.338821	0.338888	1.00	5.70
23193507	208.703445	49.226929	0.473158	0.473174	3.40	4.60
23653629	209.116013	50.653641	0.442052	0.442055	2.40	4.40
24019356	208.649506	50.454273	0.517473	0.517460	1.50	4.60
24020106	209.853088	5.836339	0.542397	0.542396	2.90	4.50
24216004	209.385406	6.251467	0.382077	0.381912	1.90	7.80
880588	208.532242	6.762656	0.600138	0.600134	1.20	2.40
1212611	208.592422	6.144436	0.630896	0.630893	0.90	1.20
1876491	209.131027	5.983884	0.760128	0.760123	1.20	1.20
3048546	209.125137	-4.194337	0.656287	0.656293	1.00	1.30
5272753	208.115189	-4.847239	0.485827	0.485831	0.90	1.60
8610884	208.744736	-4.852155	0.592421	0.592429	2.20	4.30
8907563	209.521454	-3.322183	0.513164	0.513164	1.10	4.60

LINEAR ID	RA	DEC	LINEAR period	ZTF period	LINEAR chi-2	ZTF chi-2
9852554	208.390961	-4.619442	0.651339	0.651367	1.00	4.50
9961135	209.178848	52.903030	0.590896	0.590891	1.10	1.80
10503746	208.417831	54.266953	0.573563	0.573570	2.70	1.90
21948290	209.862518	56.455978	0.511127	0.511115	2.30	2.40
23596342	209.988663	56.828396	0.602841	0.602846	1.20	2.90
23898397	121.150764	42.483574	0.563018	0.562989	1.60	3.50
1882088	208.323578	58.245502	0.315984	0.316041	4.00	1.50
2936953	208.351578	57.226521	0.328746	0.328733	2.70	1.30
3219035	209.858856	60.601982	0.326746	0.326509	3.90	2.60
4320492	168.062149	65.801857	0.361005	0.360942	3.70	1.80
8036191	208.732498	59.448402	0.363860	0.363893	2.20	1.60
10420063	209.945786	61.264187	0.487395	0.487394	4.20	3.70
10662468	209.124405	61.076996	0.445180	0.445167	3.60	1.80
21688272	209.311371	62.800976	0.304803	0.304790	2.30	1.80
2714034	168.354202	65.678604	0.610868	0.610800	1.50	1.20
5592590	208.440872	65.857277	0.346945	0.346980	1.20	1.10
8799313	208.821136	7.846983	0.327560	0.327542	1.10	1.60